Transport of inertial particles in a turbulent premixed jet flame

2011 J. Phys.: Conf. Ser. 318 092008

(http://iopscience.iop.org/1742-6596/318/9/092008)

Transport of inertial particles in a turbulent premixed jet flame

F Battista[1], F Picano[1], G Troiani[2] and C M Casciola[1]

[1]Dip. di Ingegneria Meccanica e Aerospaziale, Sapienza University, via Eudossiana 18, 00184, Rome Italy
[2]ENEA C.R. Casaccia, via Anguillarese 301, 00123, Rome Italy

E-mail: guido.troiani@enea.it

Abstract. The heat release, occurring in reacting flows, induces a sudden fluid acceleration which particles follow with a certain lag, due to their finite inertia. Actually, the coupling between particle inertia and the flame front expansion strongly biases the spatial distribution of the particles, by inducing the formation of localized clouds with different dimensions downstream the thin flame front. A possible indicator of this preferential localization is the so-called Clustering Index, quantifying the departure of the actual particle distribution from the Poissonian, which would correspond to a purely random spatial arrangement. Most of the clustering is found in the flame brush region, which is spanned by the fluctuating instantaneous flame front. The effect is significant also for very light particles. In this case a simple model based on the Bray-Moss-Libby formalism is able to account for most of the deviation from the Poissonian. When the particle inertia increases, the effect is found to increases and persist well within the region of burned gases. The effect is maximum when the particle relaxation time is of the order of the flame front time scale. The evidence of this peculiar source of clustering is here provided by data from a direct numerical simulation of a turbulent premixed jet flame and confirmed by experimental data.

1. Introduction

Particle-laden reactive flows are frequently found in many fields of engineering such as solid-propellent rockets or liquid-fuel engines or soot formation in combustion chambers, see e.g. (Simmons, 2000).

The particle dynamics is discussed in several incompressible flow configurations with the aim to understand localization phenomena such as turbophoresis in wall bounded flows or preferential accumulation and clustering in the small scales of turbulence (e.g. Goto & Vassilicos, 2006; Bec *et al.*, 2007; Wang *et al.*, 2000; Gualtieri *et al.*, 2009; Marchioli & Soldati, 2002; Picano *et al.*, 2009; Eidelman *et al.*, 2009).

Despite its relevance, much less effort was made to understand inertial particle dynamics in turbulent reactive flow. Purpose of the present paper is to discuss recent numerical and experimental data (Picano *et al.*, 2010) concerning the effect of a turbulent flame on the statistical properties of inertial particle spatial distributions. The issue may be relevant for evaluating combined inertia/combustion effects on particle collision and coalescence.

A suitable Stokes number St_{fl}, called the flamelet Stokes number, expressed in terms of the characteristic time scale of the flame front, is found to properly parametrize the particle

dynamics (Picano *et al.*, 2010). On top of the expected average density reduction across the front, we find that the front fluctuation leads to strong intermittency of the particle population. To this end, the clustering index (Kostinski & Shaw, 2001) and the radial distribution function $g(l)$ (Bec *et al.*, 2007) is used to quantitatively address the particle trend to get concentrated in clusters of variable dimensions depending on their inertia. As main conclusion we find that particles manifest a strong tendency towards anomalous clustering in the region spanned by the instantaneous turbulent flame front. The effect is found to peak at order one flamelet Stokes number.

2. Methodology

Particle dynamics in a turbulent premixed flame is studied by means of an Eulerian Direct Numerical Simulation (DNS) of a turbulent Bunsen burner coupled with a Lagrangian solver for particle evolution.

The Eulerian algorithm discretizes the Low-Mach number formulation of the Navier-Stokes equations in a cylindrical domain which describe a low Mach number flow with arbitrary flame-induced density variations, neglecting acoustics effects(Picano *et al.*, 2010).

The chemical kinetics is given by a simple one-step irreversible reaction transforming premixed fresh mixture R into exhaust gas, or combustion products P, with an Arrhenius model for the reaction rate. The DNS reproduces the flame in a premixed Bunsen burner with diameter-based Reynolds number $Re_D = U_0 D/\nu_\infty = 6000$, with U_0 the bulk velocity and diameter $D = 20\,\mathrm{mm}$.

The parameters of the simulation correspond to a lean premixed methane-air Bunsen flame (equivalence ratio $\phi \sim 0.7$, $T_b/T_u = 5.3$), with heat capacity ratio $\gamma = c_p/c_v = 1.3$, and temperature dependent viscosity according to Sutherland's law, $\mu \propto \sqrt{T}$. The ratio of laminar flame speed to the bulk velocity at jet exit is $\mathrm{S}_{fl}/U_0 \simeq 0.05$, with laminar flame-thickness $\delta_{lf} \simeq 0.019\,D$.

The computational domain, $[\theta_{max} \times R_{max} \times Z_{max}] = [2\pi \times 6.2D \times 7D]$, is discretized by $N_\theta \times N_r \times N_z = 128 \times 201 \times 560$ nodes with radial mesh stretching for accurate resolution of the shear layer and of the instantaneous flame front ($4 \div 5$ points within the instantaneous flame thickness), see (Picano *et al.*, 2010) for details and tests.

Concerning the particulate phase, small spherical particles are considered, neglecting inter-particle collisions and force feedback on the fluid as appropriate for dilute suspensions (Balachandar & Eaton, 2010). Under these assumptions, with particle mass density much larger than the fluid, $\rho_p/\rho_f \gg 1$, the equations describing the dispersed particle dynamics read (Maxey & Riley, 1983):

$$\begin{cases} \dot{\vec{x}} = \vec{v} \\ \\ \dot{\vec{v}} = \dfrac{\vec{u}(\vec{x},t)|_{\vec{x}=\vec{x}_p} - \vec{v}}{\tau_p} \end{cases} \tag{1}$$

where $\vec{x}_p$ and $\vec{v}$ are the particle position and velocity, respectively, while $\vec{u}(\vec{x},t)|_{\vec{x}=\vec{x}_p}$ is the fluid velocity at the particle position.

The relaxation time $\tau_p = d_p^2 \rho_p/(18\nu\rho_f)$ represents the particle response delay to fluid velocity fluctuations (here d_p is the particle diameter).
In order to sharply focus on the effect of particle inertia in turbulent premixed flames we neglect the thermophoretic force which may be shown to be negligible unless the particles are extremely tiny (Troiani *et al.*, 2009).

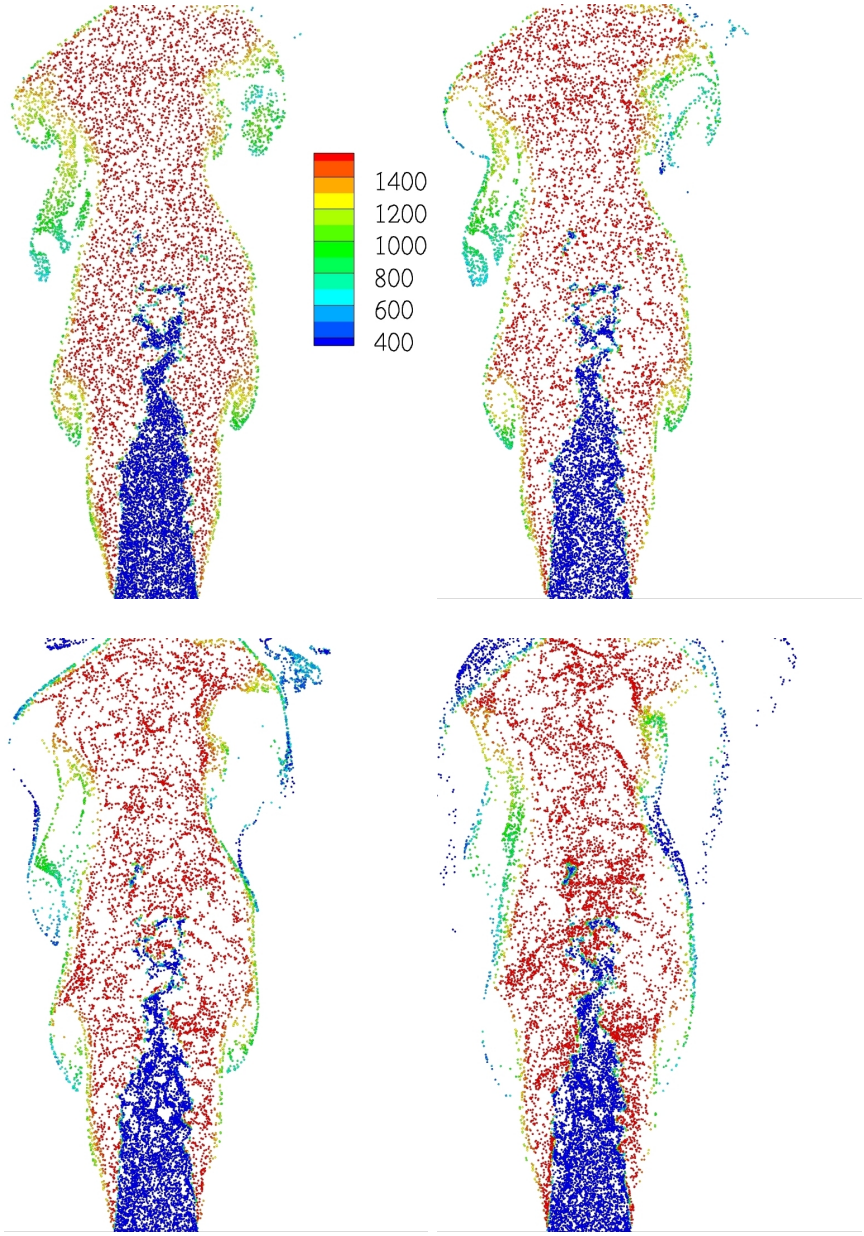

Figure 1. Instantaneous particle configuration in a thin slice of width $R/20$ through the axis. Top-left: $St_{fl} = 0.022$; Top-right: $St_{fl} = 0.54$; Bottom-left $St_{fl} = 2.16$; Bottom-right $St_{fl} = 8.65$. Colors encode the fluid density at particle positions, see legend.

Particles evolve by a Lagrangian tracking method which integrates equation (1) by means of the same Runge-Kutta scheme used for the fluid phase. Interpolation of fluid velocity at particle positions is done by using second order Lagrangian polynomials.

The proper parameter controlling particle dynamics is a suitably defined Stokes number, ratio of the particle relaxation time to the relevant time scale of the flow. In turbulent premixed combustion the strong fluid acceleration due to the abrupt thermal expansion across the flame front induces the most critical time scale (Picano *et al.*, 2010) that can be defined in terms of the laminar characteristics of the front, i.e., $\tau_{fl} = \delta_{fl}/\Delta u_{fl}$ where δ_{fl} is the thermal thickness of the laminar flame and Δu_{fl} the velocity jump across the front. The thermal

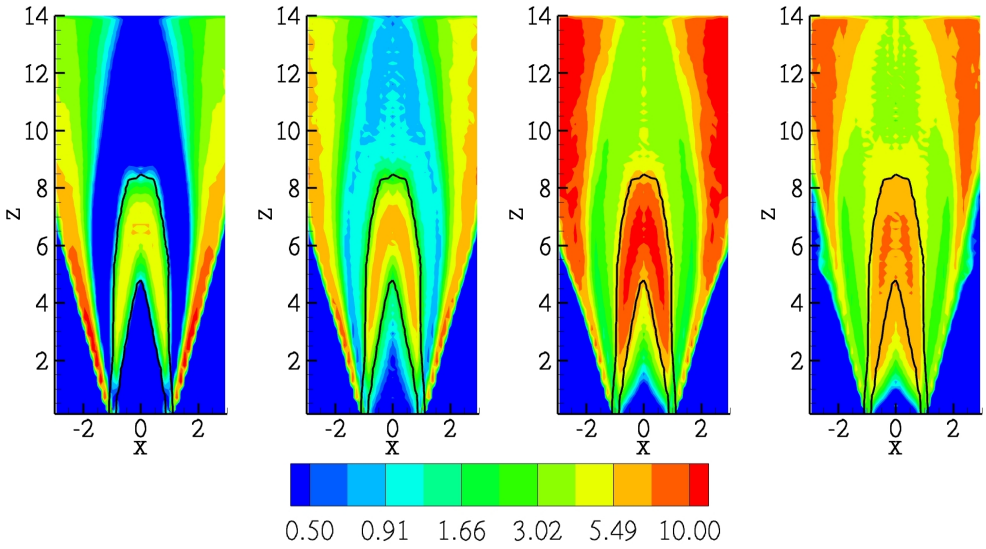

Figure 2. Clustering index contours K, eq. (3). From left to right $St_{fl} = 0.022$, $St_{fl} = 0.54$, $St_{fl} = 2.16$ and $St_{fl} = 8.65$. The clustering index is evaluated on control volumes of characteristic size $\ell = 0.125\,R$. The solid lines ($Y_R/Y_R^0 = 0.05$ and $Y_R/Y_R^0 = 0.95$) delimit the flame brush.

thickness can be estimated as $\delta_{fl} = (T_b - T_u)/|\nabla T|_{sup}$, where T_b and T_u are the temperature of burned and unburned mixtures respectively, with $|\nabla T|_{sup}$ the maximum temperature gradient modulus. Note that the thickness of the instantaneous flame where the actual reaction occurs is typically larger than δ_{fl}. Across the flame thermal expansion drives a velocity jump $\Delta u_{fl} = \mathrm{S}_{fl}\,(T_b/T_u - 1)$, with S_{fl} the laminar flame speed. In these conditions the relevant Stokes number controlling particle dynamics can be taken as (Picano *et al.*, 2010)

$$St_{fl} = \frac{\tau_p\,\mathrm{S}_{fl}\,(T_b/T_u - 1)}{\delta_{fl}}\ . \tag{2}$$

We stress that the flamelet Stokes number defined above depends on the particle relaxation time τ_p and on thermo-chemical properties of the flame, namely temperature ratio T_b/T_u and flamelet thickness δ_{fl}.

Four particle populations are considered to mimic a laboratory Bunsen premixed flame seeded with alumina particles ($\rho_p = 4000\ kg/m^3$) with diameters $d_p = 1\mu m$, $d_p = 5\mu m$, $d_p = 10\mu m$, $d_p = 20\mu m$. In the four cases the flamelet Stokes numbers are respectively $St_{fl} = 0.022$, $St_{fl} = 0.54$, $St_{fl} = 2.16$, $St_{fl} = 8.65$.

Particles are introduced in the field at a fixed rate with homogeneous distribution at the jet inlet section with velocity matching the local fluid. About six million particles are evolved in the simulation.

The simulation run for $30\,D/U_0$ to achieve the statistical steady state before collecting one hundred sample fields, separated by $0.125\,D/U_0$, for statistical analysis.

3. Clustering index

3.1. Numerical analysis

Figure 1 provides an instantaneous configuration of the four particle populations. Colors denote the fluid temperature at particle positions to help detecting the flame front. The huge variations in the particle concentration between fresh and exhaust gas regions is induced by the sudden

expansion due to heat release. Due to their inertia, particles are not able to follow the abrupt fluid acceleration. This effect is not confined to the front proximity and, depending on particle mass, it can influence the particle distribution well into the burned gas region.

Particle clusters is especially apparent in the burned gas region for particles with $St_{fl} = 0.54$ and 2.16, see figure 1. The lightest particles are more evenly distributed both in the burned and unburned regions recovering the tracer-like behavior characterized by a sharp jump of the particle number density across the front.

Particle segregation can be measured by the deviation of the actual particle distribution with respect to the randomly distributed independent positions. These reference conditions are expressed by the Poisson distribution which gives the probability $p(n)$ to find n particles in a certain domain Ω of volume ΔV. Since in Poissonian processes the variance $\sigma_n^2 = \overline{(n-\bar{n})^2} = \overline{(\delta n)^2}$ equals the mean value $\bar{n}$, the particle segregation can then be quantified by the clustering index (Kostinski & Shaw, 2001)

$$K = \frac{\overline{(\delta n)^2}}{\bar{n}} - 1 \tag{3}$$

which vanishes identically for Poissonian distributions. For deterministic systems where the number of particles found in ΔV systematically equals $\bar{n}$ the clustering index attains its minimum value -1. On the contrary, where particles aggregate in clusters, the variance of the number of particles found in ΔV is larger than the mean value, resulting in a positive clustering index, $K > 0$. For non-homogeneous systems the clustering index becomes a scalar field $K(\vec{x})$.

The clustering index for each particle population is shown in figure 2. The region spanned by the instantaneous flame front is called the flame brush. The clustering index K is positive in the flame brush and in the outer region of the jet. In the outer region the increased value of K is indeed induced by the intermittency of the boundary between the hot jet seeded with particles and the external, particle-free, cold environment. Peculiarly, even tiny particles, $St_{fl} = 0.022$, which behave like tracers under every respects, show large values of K in the flame brush region. Actually while clustering of finite mass particles is more or less expected, this behavior of tracer-like particles needs being properly understood before the clustering properties of finite mass particles are addressed.

A model for this unexpected behavior can be developed starting from the Bray-Moss-Libby (BML) description of flamelet (Bray *et al.*, 1985) where the field is decomposed in two nearby regions, pertaining to burned ($c = 1$) and unburned ($c = 0$) gases respectively, separated by a thin instantaneous front.

Assuming that for vanishing flamelet Stokes, the particle distribution is given by a Poissonian pdf $p(c)$ both in the burned and unberned regions, thought with different mean values. This assumption, exact for tracers, is reasonably accurate also for sufficiently small particles ($St_{fl} \ll 1$).

As anticipated, in the flamelet context, the state of the mixture is either $c = 0$ (unburned) or $c = 1$ (burned), and the probability distribution for the state is $p(\vec{x}; c) = \alpha(\vec{x})\delta(c) + [1 - \alpha(\vec{x})]\delta(1 - c)$, where δ denotes the Dirac function, and $\alpha = 1 - \bar{c}$ the probability to find the unburned state at $\vec{x}$. The average particle number in the control volume in each of the two states, $\overline{n_u}$ and $\overline{n_b}$, for the unburned $c = 0$ and burned $c = 1$ state, respectively can be expressed in terms of expansion ratio

$$\tau = T_b/T_u = \overline{n_u}/\overline{n_b}. \tag{4}$$

The probability to find n particles in the control volume at $\vec{x}$ as a function of the instantaneous progress variable c, then reads

$$p_c(\vec{x}; c, n) = \alpha(\vec{x})\delta(c)p[n; \overline{n_u}] + (1 - \alpha(\vec{x}))\delta(1 - c)p[n; \overline{n_b}] \tag{5}$$

Starting from the equation (5) we can express the first and second order moments of the particle number pdf,

$$\bar{n}(\vec{x}) = \alpha(\vec{x})\overline{n_u} + [1-\alpha(\vec{x})]\overline{n_b} \tag{6}$$

$$\overline{n^2}(\vec{x}) = \alpha(\vec{x})\overline{n_u^2} + [1-\alpha(\vec{x})]\overline{n_b^2}. \tag{7}$$

Introducing equations (4), (6) and (7) into the definition of clustering index (3), it follows

$$K_0(\vec{x}) = \frac{\overline{n}_u}{\tau}\frac{\bar{c}(\vec{x})[1-\bar{c}(\vec{x})]\,(\tau-1)^2}{\bar{c}(\vec{x})+\tau[1-\bar{c}(\vec{x})]}. \tag{8}$$

Hence, according to the flamelet model, the clustering index of purely Lagrangian tracers deviates from zero in the flame brush where $0 < \bar{c} < 1$, to vanish in the burned and unburned region where the statistics comes back to Poissonian.

Relation (8) highlights that for light particles, a positive clustering index, $K_0 > 0$, is mainly due to the fluctuation of the thin flame front which locally induces an intermittent state switching between unburned (higher particle concentration) and burned (lower concentration) conditions. The intermittency results in local density fluctuations which correspond to $K_0 > 0$. It is worth emphasizing that $K_0 > 0$ is here due to the alternation between two purely Poissonain states, which show no clustering when taken separately. As we will see this effect occurs also for inertial particles where the phenomenology is much more rich due to flame front fluctuations/corrugations interacting with the typical response time of the particle.

When the particle inertia is significant, the particle interaction with the flame introduces additional effects depending on St_{fl}, see figure 2. The clustering index is in general larger than the tracers'. The peak clustering occurs within the flame brush, though a significant value is also found in the burned gas region. Indeed the maximum peak clustering intensity takes place for particles with $St_{fl} = 2.16$. The observation that peak clustering is achieved at flamelet Stokes numbers order one confirms that St_{fl} is the actual parameter controlling particle localization effects in turbulent premixed flames.

The model for tracers, equation (8), can be extended to inertial particles by assuming that the fluctuating flame front separates two states, now both non Poissonian and characterized by $\bar{n}_{u,b}$ and $\overline{\delta n_{u,b}^2}$ (hence $K_{u,b} = \overline{\delta n_{u,b}^2}/\bar{n}_{u,b} - 1$) for the unburned and burned mixtures, respectively. From the flamelet model, the same procedure used for equations (6) and (7) yields

$$\overline{\delta n^2} = (1-\bar{c})\overline{n_u}K_u + \overline{cn_b}K_b + \bar{c}(1-\bar{c})(\overline{n_u} - \overline{n_b})^2 + \bar{n}\,.$$

Hence the clustering index becomes,

$$K = K_0 + \frac{K_u\tau + (K_b - K_u\tau)\bar{c}}{(1-\tau)\bar{c}+\tau} \tag{9}$$

where K_0 is the clustering index for tracers with a maximum in the flame brush, while the second contribution accounts for the effect in the flame brush of the clustering occurring in the pure states ($K_{u,b}$). In the range $0 \le \bar{c} \le 1$, the latter is a monotone function of $\bar{c}$.

In fact, the data we have available show that $K - K_0$ do exhibit a maximum inside the flame brush, suggesting that additional effects should be present and that the fluctuation between two pure non-Poissonian states is not the origin of this behavior.

3.2. The radial distribution function

In alternative to the description in terms of deviation from the reference Poissonian distribution, particle clustering is often conveniently described in terms of the scale-dependent radial

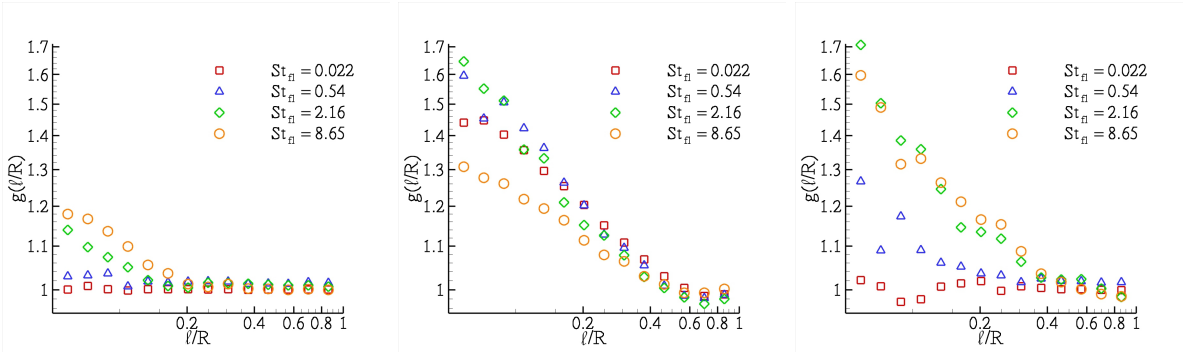

Figure 3. Radial Distribution Function $g(\ell)$ for the particles populations at different axial distances: from left: $z = 3R$, $z = 7R$, $z = 12R$.

distribution functions $g(\ell)$, see Bec *et al.* (2007) and Gualtieri *et al.* (2009). It provides the probability to find a couple of particles with distance in the interval $[\ell, \ell + d\ell]$ normalized with the probability that would result from a purely random spatially delta-correlated arrangement of particles. In presence of small scale clustering the probability to have a second particle in the vicinity of a previous one is much larger than that expected on the basis of the delta-correlated distribution, hence the increase above one of $g(\ell)$ at the given scale. Classically, the radial distribution function is introduced in the context of homogeneous flows as

$$g(\ell) = \frac{1}{4\pi\ell^2} \frac{d\mathcal{N}(l)}{d\ell} \frac{V^T}{\mathcal{N}^T}, \tag{10}$$

where $\mathcal{N}^T = 0.5N(N-1)$ is the total number of pairs in the system of volume V^T and $\mathcal{N}(\ell)$ is the number of pairs in the system with distance less or equal to ℓ.

The radial distribution function $g(\vec{x}, \ell)$ at three different axial positions along the jet is presented for the four particle populations taking $\vec{x}$ on the jet axis. The three positions are selected to check the particle system in the reactants $z = 3R$, in the flame brush $z = 7R$ and in the product region $z = 12R$, respectively (panels from left to right in the figure 3 where the separation ℓ is normalized with the nozzle radius R). The three positions are best visualized in figure 2 where the thick lines denote the boundary of the flame brush.

As due, the generalized definition of radial distribution function complies with the requirement that it should tend to one for large ℓ/R. In the reactants (left panel of figure 3, $z = 3R$) $g(\ell/R)$ slightly exceeds one at small scales $\ell/R \ll 1$. The slope of the logarithmic plot increases with the Stokes number. Since the present values of the flamelet Stokes number correspond to Kolmogorov-Stokes numbers in the range $St_\eta \in [10^{-2}, 4.0]$ the above observation are entirely consistent with the picture of particle clustering in cold flows, either isotropic (Bec *et al.*, 2007) or shear dominated (Gualtieri *et al.*, 2009). The effect on the instantaneous configurations is clearly appreciated in figure 1 by looking at the darker areas of largest particle density corresponding to the fresh gases.

The middle panel of figure 3 more or less corresponds to the average position of the flame tip, $z = 7R$. Again the generalized radial distribution function $g(\vec{x}, \ell/R)$ tends to unity at large scales despite of the strong inhomogeneity of the particle distribution. Noteworthy $g(\vec{x}, \ell/R)$ gives evidence of substantial clustering for all the particle populations, also for lightest particles $St_{fl} = 0.022 - 0.54$. Its small scale value considerably exceeds one with a significantly increased slope. Particles with $St_{fl} = 2.16$ present the steeper slope, consistently with their typically larger clustering index K, as inferred from figure 2.

Further downstream, at $z = 12R$ the lightest particles tend to recover a more regular spatial arrangement, closely resembling a spatially delta-correlated distribution. The visual inspection

of the instantaneous configurations in figure 1 confirm this trend showing a reduced occurrence of particle clusters. The heaviest particles instead still show a steep slope and the instantaneous configuration clearly manifest distributions characterized by intense aggregates separated by definite voids.

Overall the clustering intensity is found to achieve its maximum in the flame brush consistently with the indications provided by the clustering index field of figure 2. We conclude that combustion has a strong influence on particle clustering.

3.3. Experimental analysis

The results discussed in the context of DNS can be extended to actual experimental data. To this purpose an air/methane stoichiometric mixture, seeded with alumina ($\rho_p \simeq 4000$ Kg/m^3) particles with diameter of 10 μm, has been injected into a Bunsen device with nozzle diameter $D = 18$ mm at Reynolds number $Re_D = 8000$. The characteristic time scale of the corresponding laminar flame front is of the order of $\tau_{fl} \simeq 0.16$ ms (Picano *et al.*, 2010) leading to a flamelet Stokes number $St_{fl} = 4.4$.

Snapshots of the particle distributions are obtained adopting a commercial PIV system based on a 532 nm, 54 mJ Nd:YAG laser with a pulse-to-pulse delay of 70 μs. As usual the laser beam goes through a cylindrical lens to generate a light sheet of thickness 0.45 mm. The camera is equipped with a 60 mm focal length lens and with a 1280×1024 pixel CCD corresponding to a field-of-view of 110.7 mm $\times$ 88.52 mm. More details on the experimental setup can be found in (Picano *et al.*, 2010; Troiani *et al.*, 2009).

The left panel of figure 4 shows the raw data corresponding to a Mie scattering image. An image analysis algorithm is used to extract the particle positions and to count the particle numbers in control volumes of dimension of $1.26 \times 1.26 \times 0.45\, mm$ ($0.14 \times 0.14 \times 0.05\, R$) centered at different positions within the field of view of the system. The box counting algorithm allows to determine the clustering index field K by evaluating for each box mean particle number and variance. The clustering index field is reported in the right panel of figure 4. An estimate of the flame brush is obtained by looking at the iso-levels of mean particle concentration. Its boundary is reported as thick black solid lines shown superimposed on the clustering index field. The typical particle density in the experiments is nearly half the value used in the DNS. The correspondence between numerics and experiments is qualitatively excellent, see figures 2 and 4,

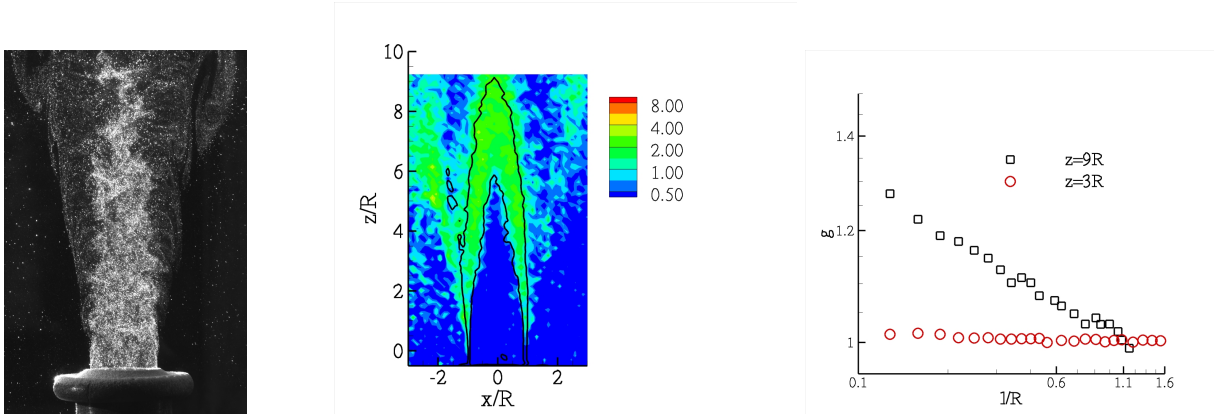

Figure 4. Experimental determination of the clustering index and radial distribution function in a Bunsen turbulent stoichiometric methane flame at $Re_D = 8000$ endowed with Alumina particles of diameter $d_p = 10\mu m$, $St_{fl} = 4.4$. Mie scattering image, left panel; clustering index, middle panel; radial distribution function at different quota, right panel.

respectively. The quantitative discrepancy is explained by considering that the clustering index depends strongly on the local particle density through the average particle number in the control volume. Considering for the factor two in the particle density between numerics and experiments we may conclude that, also in quantitative terms, the agreement is reasonable.

In the right panel of figure 4 it is reported the radial distribution function determinated from the experimental data. It is calculated on the jet axis at two different axial distances from the origin, $z = 3\,R$ and $z = 9\,R$, respectively. The general behavior of the experimental radial distribution function confirms the numerical analysis. In the unburned region, $z = 3\,R$, no relevant clustering is found leading to $g(\ell) \simeq 1$. Data pertaining to the flame brush region, $z = 9\,R$, show instead an intense clustering for these particles with $St_{fl} = 4.4$. The small differences between numerical and experimental values of $g(\ell)$ can be explained considering the slightly different conditions between numerics and experiment (Reynolds and Stokes numbers, equivalence ratio,...).

In conclusion, even the experimental data support the existence of a new source of clustering related to the interaction between the particle inertia and the wrinkled flame front.

4. Final remarks

The paper discusses several issues concerning the behavior of particles in a reacting turbulent Bunsen jet with special emphasis on the clustering which has been quantified for several particle populations in the different regions of the flow. The issue is discussed analyzing two different dataset, the former from a DNS, the latter from an experiment.

The cluster index K revealed useful to quantify the clustering by measuring the departure of particle distribution from that of a perfect random arrangement.

It is shown that the region which is mostly influenced by clustering is the flame brush. Light particles, $St_{fl} = 0.022$, deviate from the random homogeneous spatial arrangement only in the flame brush, exhibiting a Poissonian distribution both in the reactant and product regions. This behavior is perfectly captured by a model based on flamelet assumptions and tracer-like dynamics for the particles.

Increasing inertia influences the clustering process leading to a maximum clustering level in the flame brush for particles with $St_{fl} = \mathcal{O}(1)$. In this case clustering persists well beyond the flame brush and is clearly apparent in the product region. The heavier particles are too massive and are less influenced by the flame brush region, exhibiting a more uniform clustering distribution on the whole jet region.

The analysis of the scale dependence of the clustering, here exerted by the radial distribution function, confirms the behavior found by the clustering index.

Hence we argue that a new source of clustering exists in premixed reactive flows and it is related to the interaction between the particle inertia and the abrupt acceleartion induced by wrinkled flame front.

We expect that the clustering evidenced in the flame brush and in the product region could play a crucial role in coalescence processes, at the origin of particulate and soot formation. Presumably these findings could give useful hints to improve models for solid pollutant prediction in reacting environments.

Acknowledgments

We want to thank the COST Action MP0806 Particles in Turbulence for supporting the present work and CASPUR computing Consortium where the simulations were performed.

References

Balachandar, S. & Eaton, J.K. 2010 Turbulent dispersed multiphase flow. *Annual Review of Fluid Mechanics* **42**, 111–133.

Bec, J., Biferale, L., Cencini, M., Lanotte, A., Musacchio, S. & Toschi, F. 2007 Heavy particle concentration in turbulence at dissipative and inertial scales. *Physical Review Letters* **98** (8), 084502.

Bray, KNC, Libby, P.A. & Moss, JB 1985 Unified modeling approach for premixed turbulent combustion–part i: General formulation. *Combustion and flame* **61** (1), 87–102.

Eidelman, A., Elperin, T., Kleeorin, N., Hazak, G., Rogachevskii, I., Sadot, O. & Sapir-Katiraie, I. 2009 Mixing at the external boundary of a submerged turbulent jet. *Physical Review E* **79** (2), 026311.

Goto, S. & Vassilicos, J. C. 2006 Self-similar clustering of inertial particles and zero-acceleration points in fully developed two-dimensional turbulence. *Physics of Fluids* **18** (11), 115103.

Gualtieri, P., Picano, F. & Casciola, CM 2009 Anisotropic clustering of inertial particles in homogeneous shear flow. *Journal of Fluid Mechanics* **629**.

Kostinski, A.B. & Shaw, R.A. 2001 Scale-dependent droplet clustering in turbulent clouds. *Journal of Fluid Mechanics* **434** (-1), 389–398.

Marchioli, C. & Soldati, A. 2002 Mechanisms for particle transfer and segregation in a turbulent boundary layer. *Journal of Fluid Mechanics* **468** (-1), 283–315.

Maxey, M.R. & Riley, J.J. 1983 Equation of motion for a small rigid sphere in a nonuniform flow. *Physics of Fluids* **26**, 883.

Picano, F., Battista, F., Troiani, G. & Casciola, C.M. 2010 Dynamics of PIV seeding particles in turbulent premixed flames. *Experiments in Fluids* pp. 1–14.

Picano, F., Sardina, G. & Casciola, CM 2009 Spatial development of particle-laden turbulent pipe flow. *Physics of Fluids* **21**, 093305.

Simmons, F.S. 2000 *Rocket exhaust plume phenomenology*. Aerospace Press.

Troiani, G., Marrocco, M., Giammartini, S. & Casciola, CM 2009 Counter-gradient transport in the combustion of a premixed ch4/air annular jet by combined piv/oh-lif. *Combustion and Flame* **156** (3), 608–620.

Wang, L.P., Wexler, A.S. & Zhou, Y. 2000 Statistical mechanical description and modelling of turbulent collision of inertial particles. *Journal of Fluid Mechanics* **415** (-1), 117–153.